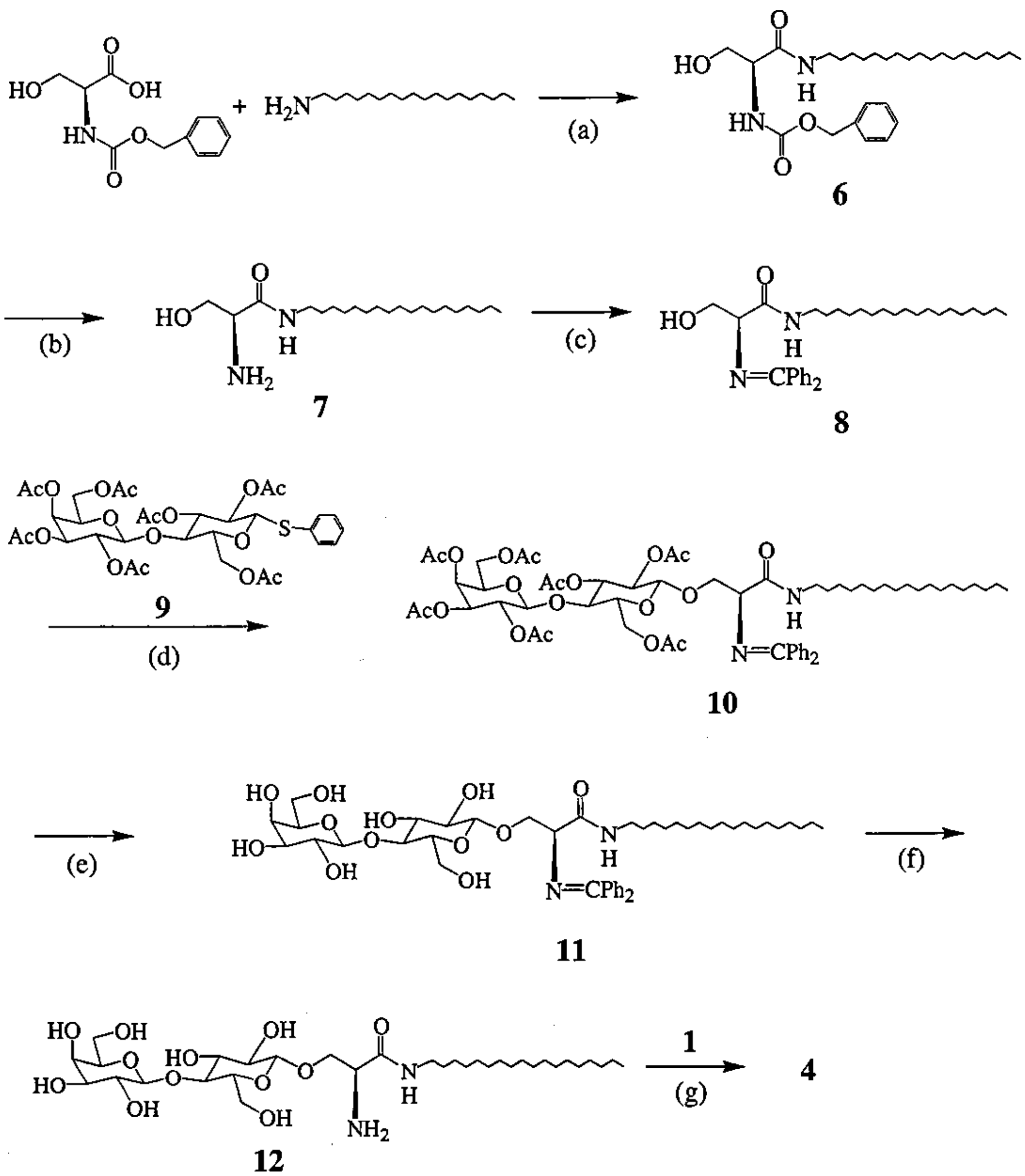


**Scheme 2.** Chemical synthesis of glycolipid **4**.
(a) EEDQ, benzene, EtOH, 25 °C, 48 h. (b) Pd–C, $H_2$, 0.32 MPa, $CH_3OH$, $CHCl_3$, 25 °C, 45 h. (c) Benzophenone imine, $CH_2Cl_2$, 25 °C, 40 h. (d) Trifluoromethanesulfonic acid, *N*-iodosuccinimide, molecular sieves 4 Å, $CH_2Cl_2$, 25 °C, 15 h. (e) Sodium methoxide, $CH_3OH$, 25 °C, 4 h. (f) Pd–C, $H_2$, $CH_3OH$, $CHCl_3$, 25 °C, 15 h. (g) *N*-Ethyldiisopropylamine, 1-ethyl-3-(3-dimethylaminopropyl) carbodiimide, $CH_3OH$, $CHCl_3$, 25 °C, 18 h.

change in UV spectra upon the addition of the proteins, showing that there was no aggregation and/or precipitation of the protein–nanoparticle complex by bridging the nanoparticles. As a control experiment, when concanavalinA (ConA), which has a specific affinity to mannose, was added to the solution of lactose-displayed nanoparticle, no change in fluorescence intensity was observed (Figure 3b). In addition, when RCA120 was added to the solution of nanoparticles prepared only from the matrix lipid **3**, no change in fluorescence intensity was observed (Figure 3c). These two control experiments clearly indicate that the fluorescent change in Figure 3a is based on the specific interaction between RCA120 and lactose residues. The concentration-dependency is summarized in Figure 3d. We attempted similar experiments using carboxylic acid-type **1** or neutral-type **2** as the matrix lipid of glyconanoparticles instead of **3**; however, not negligible change in fluorescence by non-specific binding was observed. This suggests that the use of a phosphatidylcholine-type matrix is of key importance in gaining the signals due to specific recognitions.

Binding of E-selectin, which has a single binding site for the tetrasaccharide sialyl-Lewis X ($sLe^X$), was tested using the $sLe^X$-displayed nanoparticle. E-selectin is a vascular cell surface protein which mediates leukocyte rolling on the blood vessel wall and is

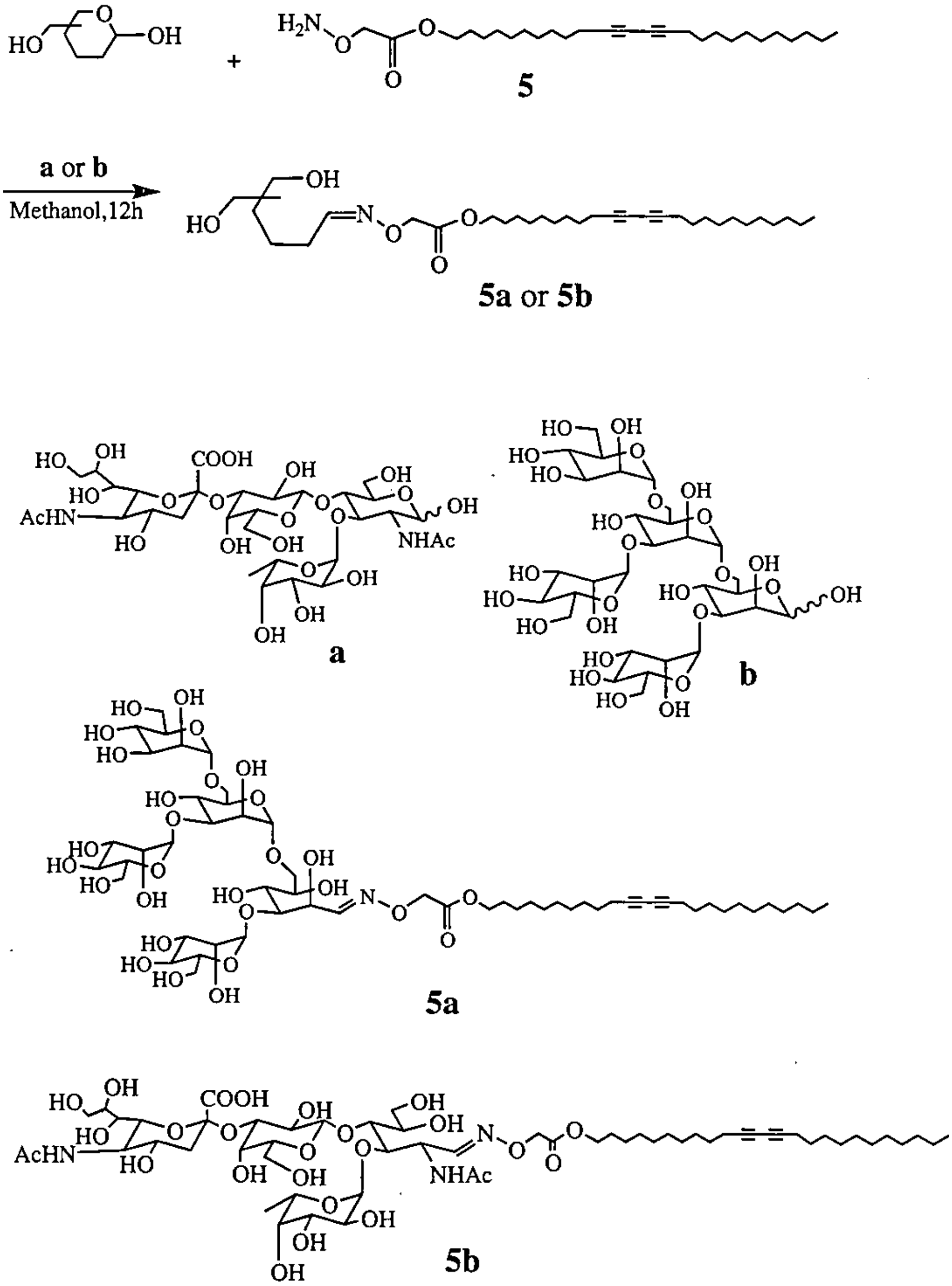


**Scheme 3.** Chemical ligation between free carbohydrates and hydroxylamine-attached lipid **5**.

responsible for an early stage of inflammatory response.[9] Thus, the sensing system of E-selectin binding to $sLe^X$ would be useful in evaluating the inhibitory effects of new blockers against E-selectin. The fluorescence of the solution of $sLe^X$-displayed nanoparticles also decreased with the increase in E-selectin concentration, whereas no change in fluorescent intensity was induced for the control nanoparticles that were synthesized from the matrix lipid alone (Figure 4a and 4b).

For the binding of concanavalinA (ConA), a lectin with a high affinity for mannose, similar results with fluorescent changes were obtained. When a lectin solution was added to the mannopentaose-displayed nanoparticles, the fluorescence intensity decreased depending upon the lectin concentration (Figure 4c and 4d). The control nanoparticles constructed using the matrix lipid **3** alone induced no change in fluorescence upon the addition of ConA, indicating there was no non-specific adsorption. In this case also, there was no change in UV spectra upon the addition of ConA at an nM range.

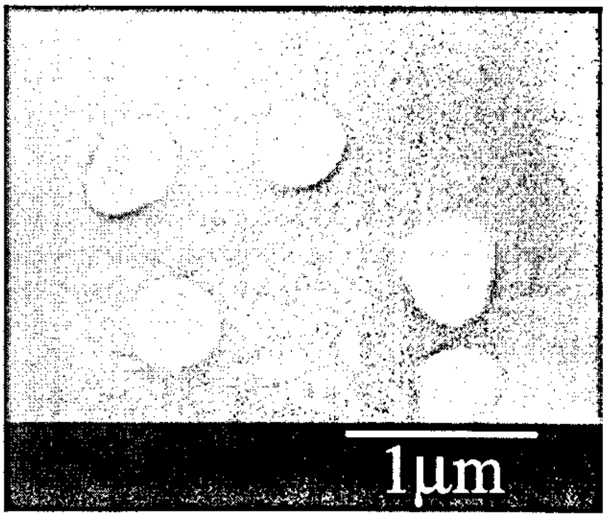


**Figure 2.** SEM image of the polymerized glyconanoparticles.

The reason for the quenching of fluorescence upon protein binding is not clear at this stage. Since the coloriometric change upon the binding of toxins seems to be caused by the reorientation of lipids and a reduction in the length of the conjugated lipid backbone due to distribution of the polymer network.[10] The reason for the change in fluorescence can be similarly speculated. Therefore, we consider that a reduction in the flexibility of the conjugated lipid backbone after the binding of proteins on the surface of the nanoparticles may lead to a decrease in fluorescence.

To prove our speculation, we modulated the UV-irradiation period to control the degree of cross-linkage in the membrane consisting of the lactose lipid **4** and matrix lipid **3**. When the irradiation period was shortened from 90 to 5 min, the fluorescent response upon the binding of RCA120 was increased [compare Fig-

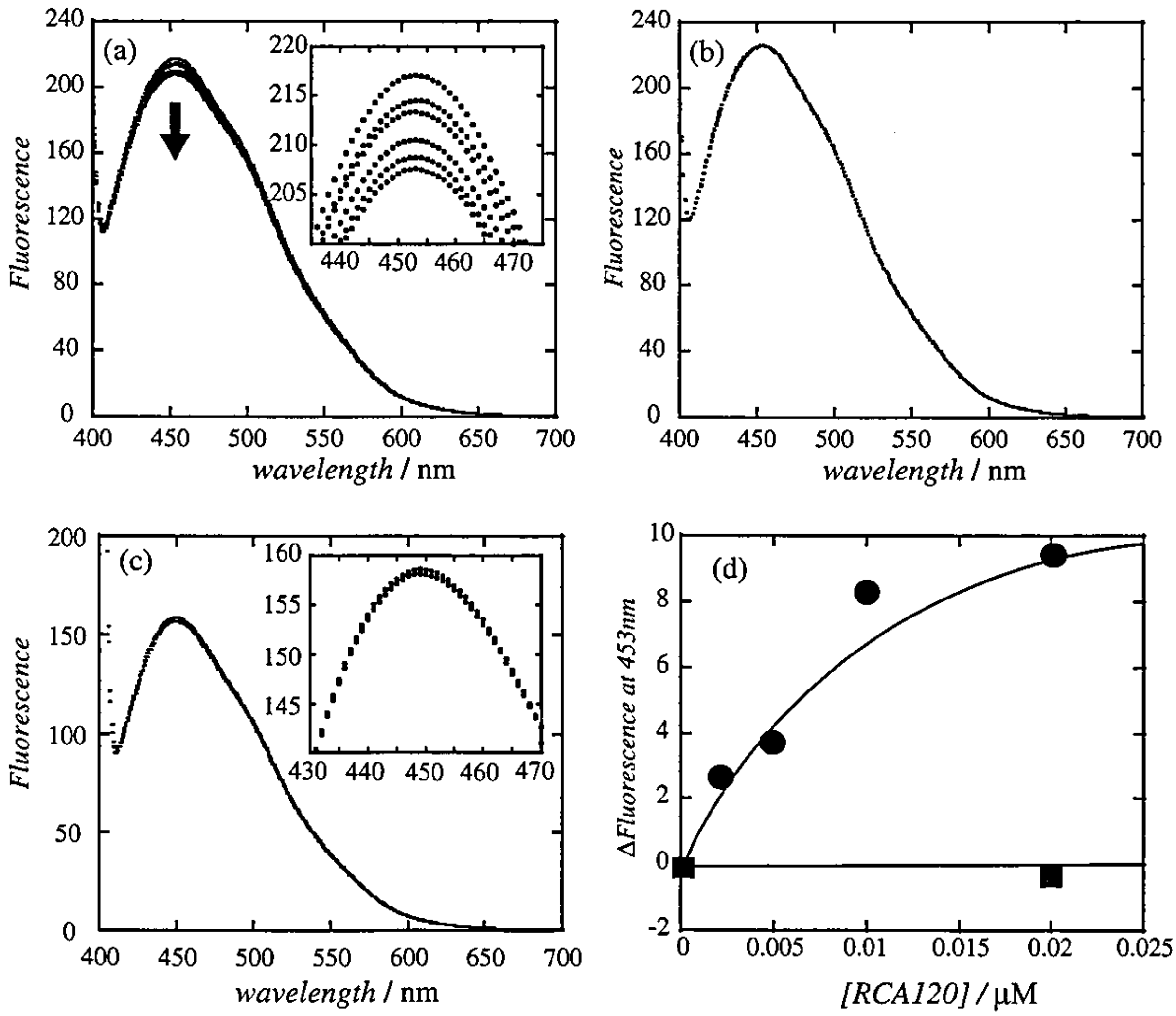


**Figure 3.** Fluorescent detection of RCA120 using nanoparticle.
(a) Change in fluorescent spectra upon the addition of RCA120 (0, 0.002, 0.005, 0.01, 0.015, 0.02 µM from top to bottom) to polymerized nanoparticle (**4**/**3**) in Tris buffer (10 mM, pH 7.4). (b) Change in fluorescent spectra upon the addition of ConA (0, 0.2 µM from top to bottom) to nanoparticle (**4**/**3**) in Tris buffer (10 mM, pH 7.4). (c) Change in fluorescent spectra upon the addition of RCA120 (0 and 0.2 µM) to nanoparticle (**3** alone) in Tris buffer (10 mM, pH 7.4). (d) Change in fluorescence as a function of lectin concentrations for figure (a): (closed circle) and figure (b): (closed square).

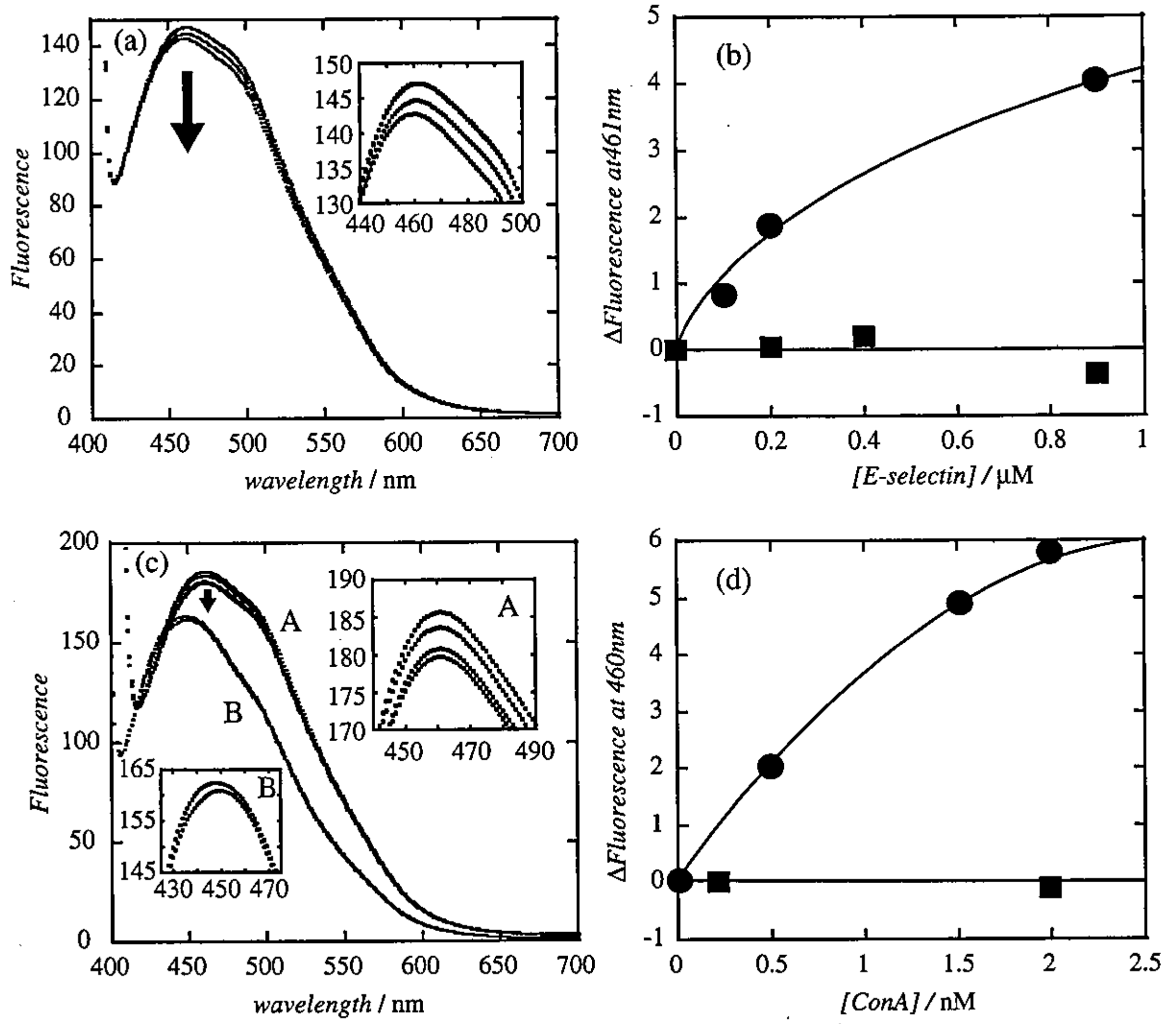


**Figure 4.** Fluorecent detection of E-selectin and ConA using glyconanoparticles.
(a) Change in fluorescent spectra upon the addition of E-selectin (0, 0.2, 0.9 μM from top to bottom) to polymerized nanoparticle (**5b**/**3**) in Tris buffer (10 mM, pH 7.4). (b) Change in fluorescence intensity as a function of E-selectin concentration. (closed circle) polymerized nanoparticle of **5b**/**3**. (closed square) polymerized nanoparticle of **3** only. (c) A: Change in fluorescent spectra upon the addition of ConA (0, 0.5, 1.5, 2 nM from top to bottom) to polymerized nanoparticle (**5a**/**3**) in acetate buffer (10 mM, pH 5.2). B: Change in fluorescent spectra upon the addition of ConA (0 and 2 nM) to polymerized nanoparticle (**3** only). (b) Change in fluorescence as a function of lectin concentration for A (closed circle) and B (closed square).

ure 3a for 90 min and Figure 5a for 5 min]. This data suggests that the enhanced response of the nanoparticles upon binding is due to the greater mobility of the loosely cross-linked diacetylene network. The effect of irradiation period on fluorescent response is summarized in Table I. When the irradiation period was increased to more than 30 min, only a low response (4%) was observed. This means that the conformation change in the ene-yne backbone of the rigid fully cross-linked membrane cannot be effectively induced during the protein binding.

As another approach to introduce flexibility to the nanoparticles, L-α-phosphatidylcholine dioleoyl (DOPC), which has a low phase-transition temperature ($T_c = 20\,°C$), was added. The fluorescence spectra after the addition of RCA120 were shown in Figure 5b and the effect of DOPC on the response is summarized in Table II. The fluorescent response of the DOPC-containing nanoparticles is two times larger than that of nanoparticles without DOPC. As the diacetylene-containing lipids are diluted in the non-polymerizable DOPC liquid phase (binding assay was carried out at 25 °C), long-ranged cross-linkage would be inhibited. Therefore, we consider that these nanoparticles have great flexibility due to the loose cross-linkage, resulting in extensive conformation change upon surface protein binding.

We next directed our attention to the monitoring of enzymatic reactions occurring on the surface of the nanoparticles. We monitored the reaction of hydrolysis of manno-oligosaccharides on the nanoparticles catalyzed by mannosidase (*Jack Bean*, Seikagaku Corporation) in acetate buffer (Figure 6). When mannosidase was added to a suspension of the mannopen-

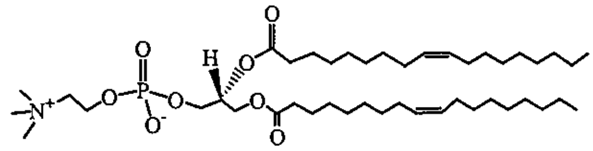

DOPC

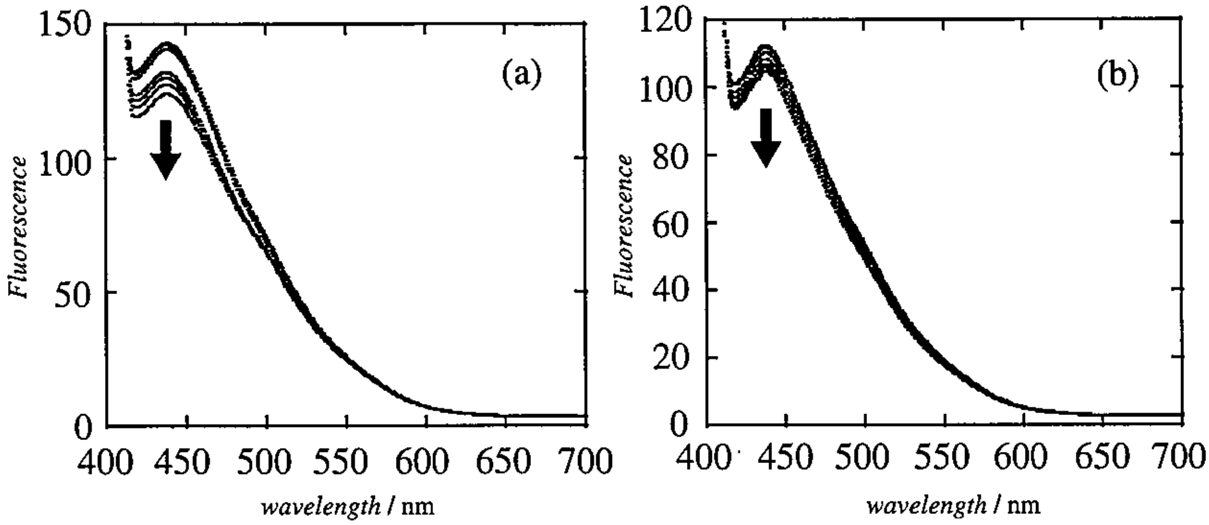


**Figure 5.** Fluorescent detection of RCA120 using nanoparticles.
(a) Nanoparticle that was prepared by UV irradiation for 5 min. (b) DOPC-containing nanoparticle (3:4:DOPC=80:10:10 mol ratio). [RCA120] = 0 to 20 nM from top to bottom.

**Table I.** Effect of UV irradiation period on the fluorescence response after the addition of RCA 120 (20 nM) to the nanoparticles (3/4)

| UV irradiation time (min) | Fluorescence response (%) |
|---|---|
| 1 | 8.5 |
| 5 | 12.9 |
| 30 | 4.0 |
| 90 | 4.4 |

**Table II.** Effect of DOPC on the fluorescence response after the addition of RCA 120 (20 nM) to the nanoparticles (3/4)

| Molecular ratio of the nanoparticles (%) | | | Fluorescence response (%) |
|---|---|---|---|
| 4 | 3 | DOPC | |
| 10 | 90 | 0 | 4.4 |
| 10 | 80 | 10 | 3.0 |
| 10 | 40 | 50 | 4.2 |
| 10 | 10 | 80 | 6.8 |

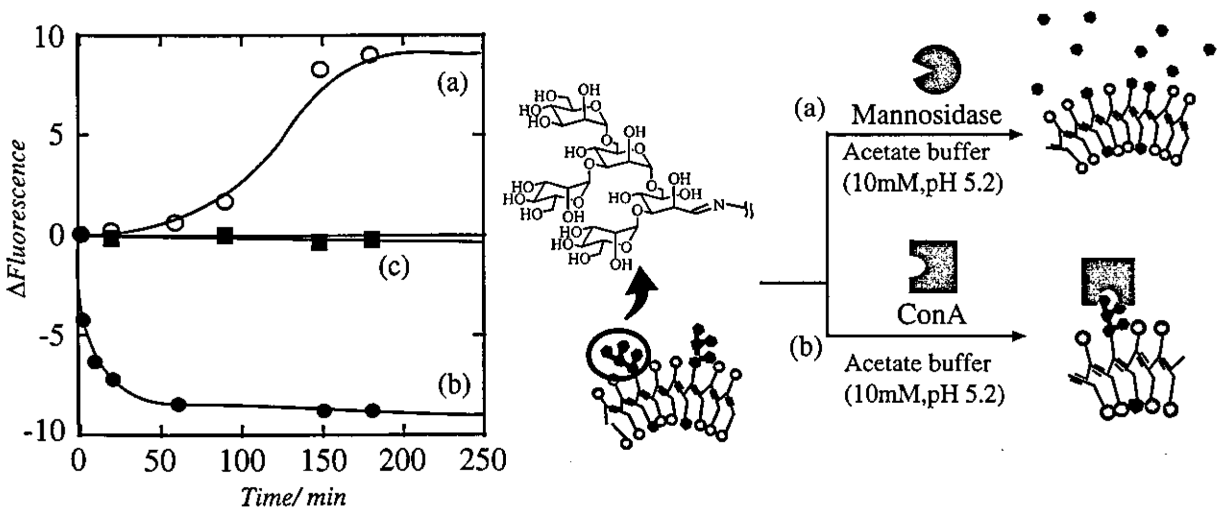


**Figure 6.** Timecourse of fluorescence intensities from mannopentaose-displayed nanoparticle. (a) After addition of mannosidase from jack bean to the nanoparticle made of 3/4. (b) After addition of RCA120 to the same nanoparticle (3/4). (c) After addition of mannosidase to the nanoparticle made of 3 alone (control).

taose-displayed nanoparticles, fluorescence increased with time. When the nanoparticles made of only matrix lipids were used, no response was observed. However, on the addition of lectins, the change in fluorescence was negative. Therefore, change in fluorescence is speculated to result from changes in stress on the diacetylene network, where the stress is increased or decreased with the binding of ConA or released of mannopentaose, resulting in respective negative or positive changes in fluorescence (see Figure 6).

## SUMMARY

The present method employing fluorescent nanoparticles allowed us to detect the binding of protein receptors too small to change common absorption spectra. Using a phosphatidylcholine-type lipid as a matrix in copolymerization reactions, the non-specific binding of proteins was excluded. The fluorescence transition depends on the quantity of proteins titrated into the solutions containing glyconanoparticles. The nanoparticles having great flexibility due to the loose cross-linkage produced large change in fluorescence. Therefore, the conformation change of the polydiacetylenic moiety induced by surface protein binding would cause the fluorescence change. It is demonstrated that the sensing system using the nanoparticles is applicable to monitoring the time-course of enzymatic reactions occurring on the nanoparticle surface. The fluorescent glyconanoparticles will be useful in the construction of sugar-arrays for the detection of unknown lectins and sugar-related enzymes.

*Acknowledgment.* This work was supported by a grant for the "Glycocluster Research & Development of Controlling Biomolecules" from NEDO. We thank Ms. Oka for ESI mass measurement at the Center for Instrumental Analysis of Hokkaido University.

## REFERENCES

1. (a) S. Chen, Q. Yu, L. Li, C. L. Boozer, J. Homola, S. S. Yee, and S. Jiang, *J. Am. Chem. Soc.*, **124**, 3395 (2002).
(b) R. J. Green, M. C. Davies, C. J. Roberts, and S. J. B. Tendler, *Biomaterials*, **20**, 385 (1999).
2. (a) H. Matsuno, K. Niikura, and Y. Okahata, *Biochemistry*, **40**, 3615 (2001).
(b) Y. Okahata, K. Niikura, Y. Sugiura, M. Sawada, and T. Morii, *Biochemistry*, **37**, 5666 (1998).
(c) Y. Ebara and Y. Okahata, *J. Am. Chem. Soc.*, **116**, 11209 (1994).
(d) T. Sato, T. Serizawa, and Y. Okahata, *Biochim. Biophys. Res. Commun.*, **204**, 551 (1994).
3. (a) W. Spevak, J. O. Nagy, D. H. Charych, M. E. Schaefer, J. H. Gilbert, and M. D. Bednarski, *J. Am. Chem. Soc.*, **115**, 1146 (1993).
(b) D. H. Charych, Q. Cheng, A. Reichert, G. Kuziemko, M. Stroh, J. O. Nagy, W. Spevak, and R. C. Stevens, *Chem. Biol.*, **3**, 113 (1996).
(c) D. H. Charych, J. O. Nagy, W. Spevak, and M. D. Bednarski, *Science*, **261**, 585 (1993).
(d) J. J. Pan and D. H. Charych, *Langmuir*, **13**, 1365 (1997).
(e) A. Berman, D. J. Ahn, A. Lio, M. Salmeron, A. Reichert, and D. H. Charych, *Science*, **269**, 515 (1995).
4. S. Okada, S. Peng, W. Spevak, and D. H. Charych, *Acc. Chem. Res.*, **31**, 229 (1998).
5. Z. Ma, J. Li, L. Jiang, J. Cao, and P. Boullanger, *Langmuir*, **16**, 7801 (2000).
6. (a) N. Nagahori, K. Niikura, R. Sadamoto, K. Monde, and S.-I. Nishimura, *Aust. J. Chem.*, **56**, 567 (2003).
(b) N. Nagahori, K. Niikura, R. Sadamoto, M. Taniguchi, A. Yamagishi, K. Monde, and S.-I. Nishimura, *Adv. Synth. Catal.*, **345**, 729 (2003).
7. (a) S. E. Cervigni, P. Dumy, and M. Mutter, *Angew. Chem., Int. Ed.*, **35**, 1230 (1996).
(b) F. Peri, P. Dumy, and M. Mutter, *Tetrahedron*, **54**, 12269 (1998).
8. E. C. Rodriguez, K. A. Winans, D. S. King, and C. R. Bertozzi, *J. Am. Chem. Soc.*, **119**, 9905 (1997).
9. (a) G. R. Larsen, D. Sako, T. J. Ahern, M. Shaffer, J. Erban, S. A. Sajer, R. M. Gibson, D. D. Wagner, B. C. Furie, and B. Furie, *J. Biol. Chem.*, **267**, 11104 (1992).
(b) K. Ley, M. Allietta, D. C. Bullard, and S. Morgan, *Circ. Res.*, **83**, 287 (1998).
10. Q. Huo, K. C. Russell, and R. M. Leblanc, *Langmuir*, **15**, 3970 (1999).

# Extra-abdominal desmoid around the shoulder joint: One of the differential diagnoses of frozen shoulder

Takuya Watanabe, MD, Naoki Suenaga, MD, and Akio Minami, MD, *Sapporo, Japan*

Extra-abdominal desmoid tumor is a type of fibromatosis derived from fascial or musculoaponeurotic structures.[3,8] When the tumor occurs around joints, movement is restricted, resulting in pain with motion. We report 3 cases of extra-abdominal desmoid tumor around the shoulder misdiagnosed as frozen shoulder.

## CASE 1

A 29-year-old woman complained of right shoulder pain and a decrease in range of motion (ROM) of the right shoulder in September 1996. She was diagnosed with frozen shoulder and treated with physical therapy and nonsteroidal antiinflammatory drugs at another clinic. However, her shoulder pain increased, and she visited our outpatient clinic in June 1997. Physical examination revealed right shoulder ROM as flexion of 140°, external rotation with the arm at the side to 0°, and internal rotation to L1. There was tenderness at the bicipital groove. Her progressive symptoms, atypical age for frozen shoulder, and reduced restriction of internal rotation suggested another cause for her shoulder symptoms. Computed tomography (CT) and magnetic resonance imaging (MRI) were performed. CT showed a round soft-tissue tumor in the subscapularis, with comparatively homogeneous density of the mass and isodensity of the subscapularis muscle (Figure 1, *A*). MRI revealed that the rotator cuff tendons were normal. On $T_1$-weighted MR images, the lesion was mostly homogeneous, and the signal intensity of the lesion was equal to that of muscle (Figure 1, *B*). The mass was enhanced heterogeneously by gadolinium. On $T_2$-weighted images, lesion tissue with a signal intensity higher than or equal to that of the subscapularis muscle was distributed heterogeneously (Figure 1, *C*).

Pathologic examination of open biopsy specimens revealed bundles of fibroblasts and large amounts of collagen, leading to a diagnosis of extra-abdominal desmoid tumor. The tumor was resected with the subscapularis muscle in April 1998. The articular capsule of the shoulder was preserved, and coracoid transplantation based on the Bristow method was performed.[5] The tumor mass was white, firm, and 50 × 40 × 40 mm in size. After surgery, the patient's right shoulder pain decreased and the shoulder ROM increased to flexion of 150° and external rotation with the arm at the side to 25°. However, she again had right shoulder pain and decreasing internal rotation in September 1999. CT and MRI revealed local recurrence of the tumor partially invading the deltoid, subscapularis, latissimus dorsi, teres major, and serratus anterior muscles (Figure 2, *A*,*B*, ). Wide resection of the recurrent tumor and a partial resection of the deltoid, subscapularis, latissimus dorsi, teres major, and serratus anterior muscles were performed. At 2 years 6 months after the second operation, there was restricted ROM with flexion of 90° and external rotation with the arm at the side to −15°. We believe that the poor ROM is the result of the extensive resection of muscles around the shoulder during the second operation.

## CASE 2

A 47-year-old woman complained of right shoulder pain and restriction of shoulder motion in March 1992. Although her shoulder was treated conservatively as frozen shoulder by a local doctor, the symptoms did not resolve. She visited our clinic in May 1997. Physical examination revealed the anterior aspect of her shoulder to contain a firm mass that was not adherent to the skin but infiltrating underlying tissue and muscle. The ROM was limited to flexion of 135°, internal rotation to the lateral thigh level, external rotation to 40°, and adduction of −20°. Her shoulder was contracted in the abduction position as a result of deltoid contracture. Tenderness was noted around the mass. We suspected that her symptoms resulted from the mass, and thus CT and MRI were performed. CT revealed that the mass had partially invaded the deltoid muscle and teres minor tendon and that those muscles were remarkably atrophic. On MRI, the margin of the mass was partially ill defined. On $T_1$-weighted images, the lesion was mostly homogeneous, and the signal intensity of the lesion was lower than that of the deltoid muscle (Figure 3, *A*). On $T_2$-weighted images, lesion tissue with high intensity and isointensity of the deltoid muscle was distributed heterogeneously (Figure 3, *B*). Pathologic examination of open biopsy tissue revealed large amounts of hyalinized collagen and fibroblasts, indicating a desmoid tumor. The tumor was widely resected with sacrifice of the infiltrated middle fibers of the deltoid muscle and teres minor tendon in July 1997. Transposition of the posterior fibers of the deltoid muscle to the anterior aspect per the Harmon method was performed,[4] and the preserved teres minor tendon was repaired by the technique of McLaughlin and Cavallero.[7] At 3 years 6 months after resection, there

From the Department of Orthopaedic Surgery, Hokkaido University School of Medicine.

Reprint requests: Takuya Watanabe, MD, Department of Orthopaedic Surgery, Hokkaido University School of Medicine, Kita-15 Nishi-7, Kita-ku, Sapporo 060-8638, Japan (E-mail: *takuya@sap-cc.go.jp*).

J Shoulder Elbow Surg 2004;13:90-4



1058-2746/2004/$35.00 + 0

doi:10.1016/S1058-2746(03)00054-5

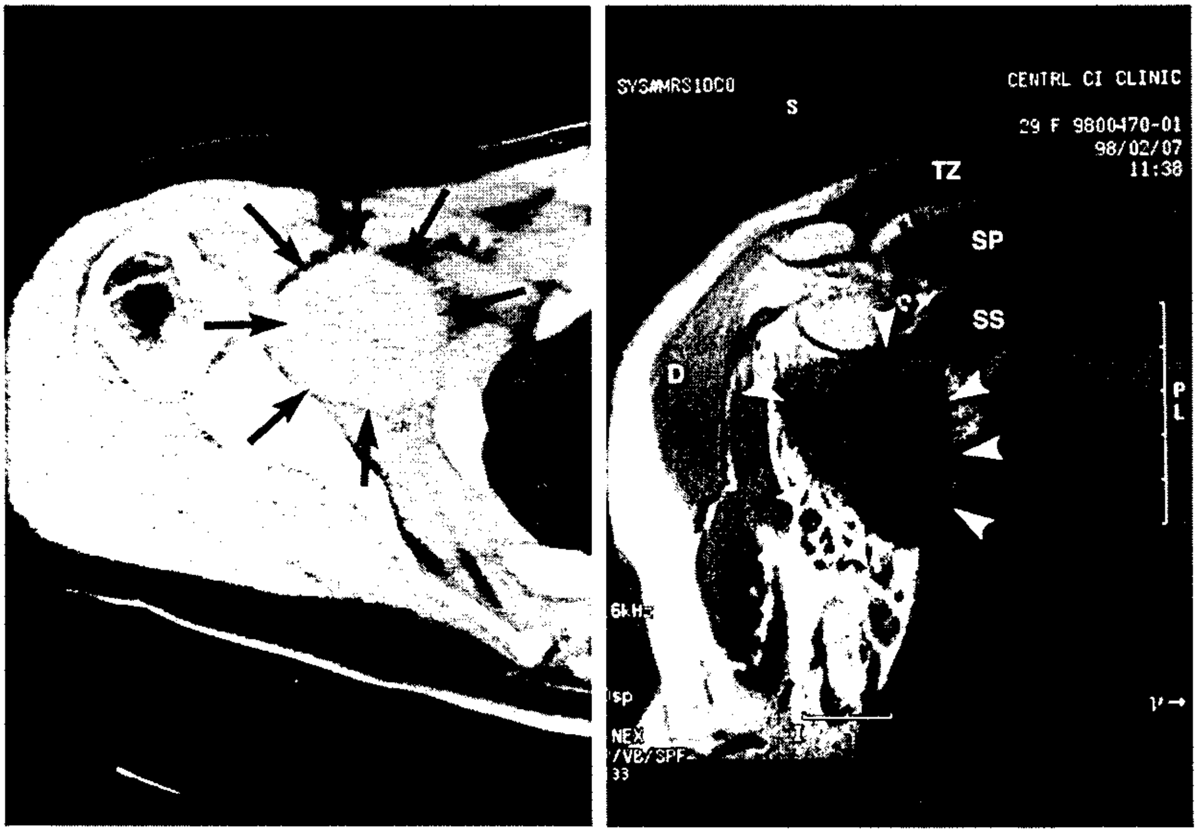


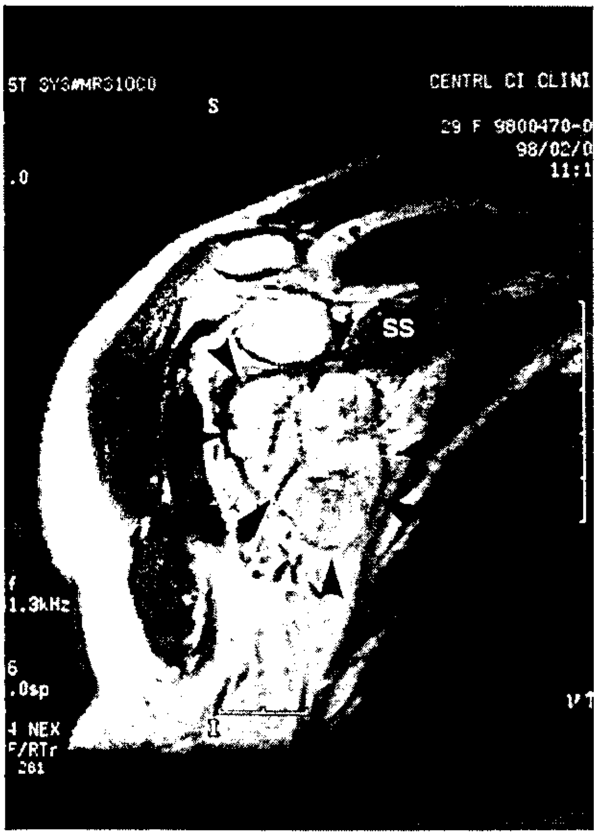


**Figure 1** **A**, CT scan of case 1 at first visit to our clinic, showing that the density of the mass (*arrows*) was comparatively homogeneous and likely equal to that of the subscapularis muscle. **B**, Coronal view of $T_1$-weighted MRI image of case 1 at first visit to our clinic. The lesion (*arrowheads*) was mostly homogeneous, and the signal intensity of the lesion was equal to that of the subscapularis muscle (*SS*). *D*, Deltoid muscle; *TZ*, trapezius muscle; *SP*, supraspinatus muscle. **C**, Coronal view of $T_2$-weighted MRI image of case 1 at first visit to our clinic. The lesion (*arrowheads*) was mixed heterogeneously, with the signal intensity higher than or equal to that of the subscapularis muscle (*SS*).

was no evidence of a local recurrence, with no marked difference in the elevation of the right shoulder compared with that of the left and with no other limitations in shoulder movement.

## CASE 3

A 57-year-old woman complained of left shoulder pain and restriction of shoulder motion in March 1999. She was diagnosed with frozen shoulder by another doctor and treated with physical therapy. However, her symptoms did not improve, and she visited our outpatient clinic in February 2000. There was a palpable mass in the supraclavicular area. The ROM was limited to flexion of 125°, abduction of 130°, external rotation to 70°, and internal rotation to T12. We believed that her symptoms resulted from the mass, and CT and MRI were performed. CT showed a mass adjacent to the subscapularis, teres minor, pectoralis major,

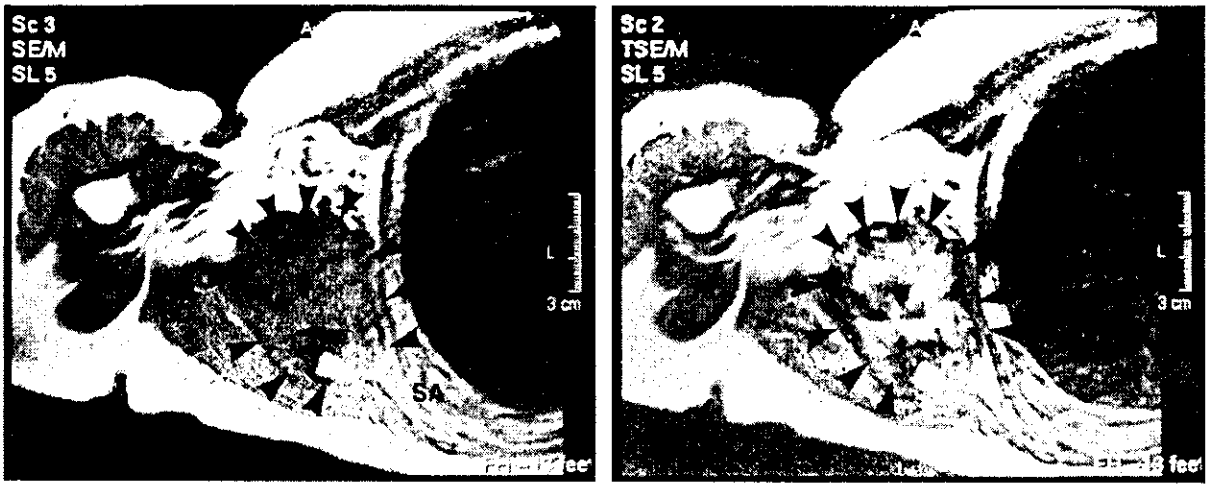


**Figure 2 A,** $T_1$-weighted MRI image of case 1 in June 2000. *Arrowheads,* Lesion; *LD,* latissimus dorsi muscle; *SA,* serratus anterior muscle. **B,** $T_2$-weighted MRI image of case 1 in June 2000. *Arrowheads,* Lesion.


**Figure 3 A,** $T_1$-weighted MRI image of case 2 in May 1997. The margin of the mass (*arrows*) was partially ill defined. The lesion was mostly homogeneous, and the signal intensity of the lesion was lower than that of the deltoid muscle. **B,** $T_2$-weighted MRI image of case 2 in May 1997. The lesion (*arrows*) with high intensity and isointensity of the deltoid muscle was distributed heterogeneously.

first to third ribs, and brachial plexus. The density of the mass was comparatively homogeneous. On $T_1$-weighted images, the lesion was mostly homogeneous, and the signal intensity of the lesion was lower than that of muscle (Figure 4, *A*). On $T_2$-weighted images, the lesion was heterogeneously distributed with a signal intensity higher than or

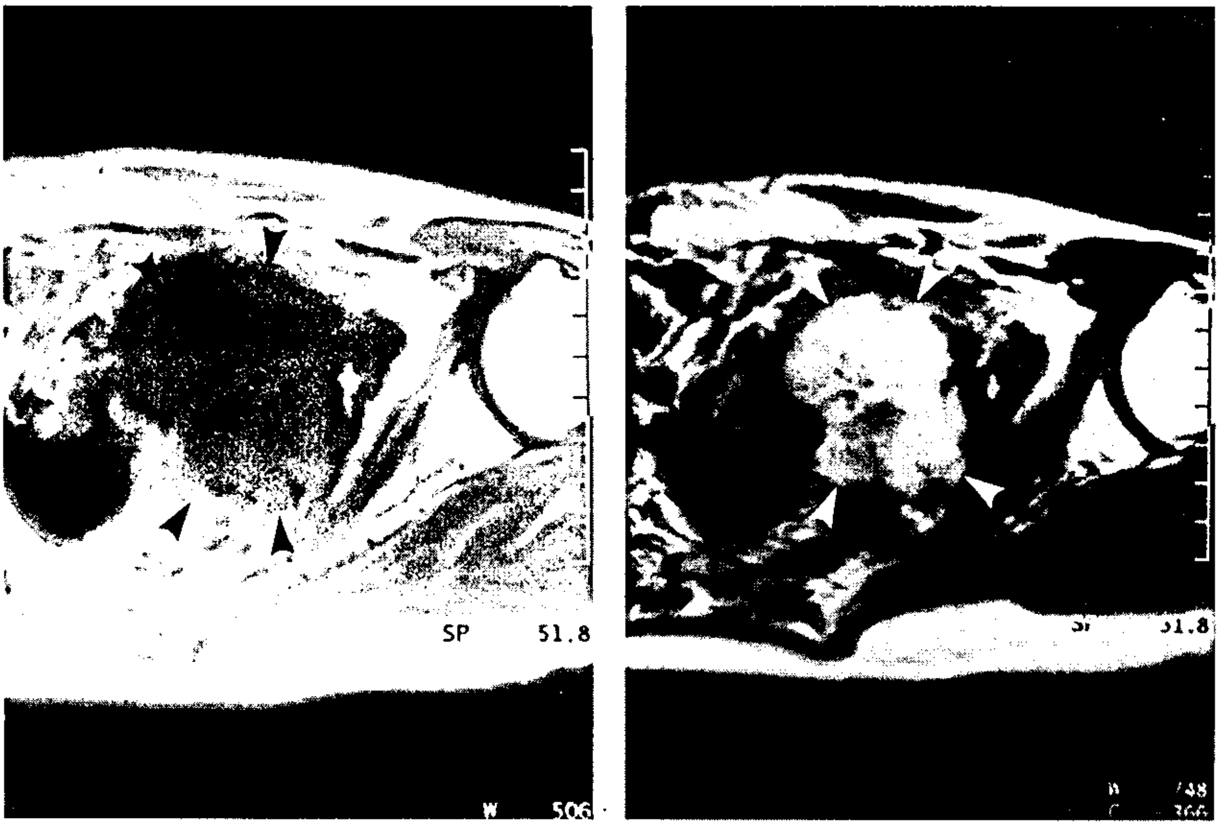


**Figure 4 A**, $T_1$-weighted MRI image of case 3 in February 2000. The lesion (*arrowheads*) was mostly homogeneous, and the signal intensity of the lesion was lower than that of the subscapularis muscle. **B**, $T_2$-weighted MRI image of case 3 in February 2000. The lesion (*arrowheads*) was heterogeneously distributed, with the signal intensity higher than or equal to that of the subscapularis muscle.

equal to that of muscle (Figure 4, *B*). The histopathologic diagnosis from biopsy specimens was desmoid tumor (Figure 5, *A,B*). In April 2000 the tumor was totally resected with the first and second ribs preserved as neurovascular bundles. Osteotomy of the left clavicle was required for tumor resection. The clavicle underwent plate fixation after tumor resection. However, bone union was delayed, and consequently, we could not allow early active and passive ROM exercises for the shoulder. Passive ROM exercises were initiated 4 weeks after surgery, and active ROM exercises were started 12 weeks after surgery. At 1 year 7 months after resection, ROM was limited to flexion of 100°, abduction of 65°, and internal rotation to L2.

## DISCUSSION

Patients complaining of shoulder pain and restriction of motion are often diagnosed with frozen shoulder, as the main symptoms of this condition are shoulder pain and restriction of shoulder ROM without trauma or infection. As differential diagnoses of the syndrome, cervical spondylosis, thoracic outlet syndrome, neuralgic amyotrophy, rotator cuff injury, arthritis of the acromioclavicular joint, and osteoarthrosis of the glenohumeral joint have been reported. However, no previous reports have documented extra-abdominal desmoid tumor around the shoulder misdiagnosed as a frozen shoulder.

Extra-abdominal desmoid tumor is a type of fibromatosis derived from fascial or musculoaponeurotic structures that gradually infiltrates muscles. The musculature of the shoulder is the most common location in which the tumor is found.[9] Although the tumor is benign and nonmetastatic, local invasion is clinically aggressive.[2] Although the standard surgical procedure for extra-abdominal desmoid tumor is wide resection,[1,6] the tumor frequently recurs and invades neighboring tissue, resulting in more functional defects. Thus, an early diagnosis is important to preserve function after wide resection of the tumor. However, swelling is often the only early symptom, rendering an early diagnosis of extra-abdominal desmoid tumor in deep lesions difficult. Nonetheless, careful examination can aid in the differential diagnosis. In case 1 the patient's age, progressive symptoms, and less restriction of internal rotation of the shoulder were atypical of frozen shoulder. In both cases 2 and 3, swelling of the shoulder was present. Thus, careful examination would most likely have resulted in an accurate diagnosis.

That being said, a diagnosis of extra-abdominal desmoid tumor is difficult with only inspection and palpation examination, making extra-abdominal desmoid tumor one of the differential diagnoses of frozen shoulder. If a patient complains of shoulder pain with restriction of motion sug-

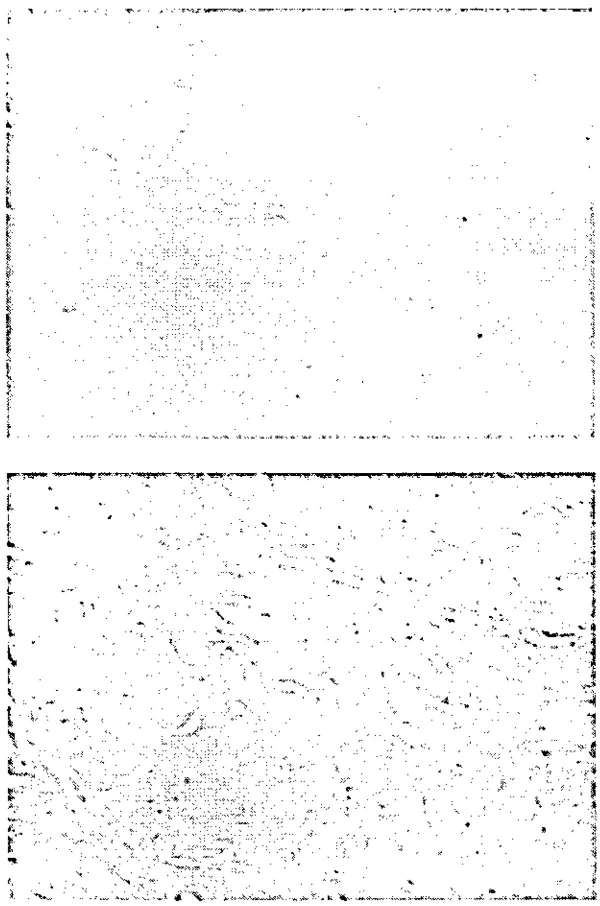

**Figure 5 A,** Hematoxylin-eosin–stained low-power view of case 3 (original magnification ×20). There were bundles of fibroblasts and large amounts of collagen. **B,** Hematoxylin-eosin–stained high-power view of case 3 (original magnification ×100). There was no atypical cell.

gestive of frozen shoulder, extra-abdominal desmoid tumor around the shoulder joint should be considered.

## REFERENCES

1. Ballo MT, Zagars GZ, Pollack A, et al. Desmoid tumor: factors and outcome after surgery, radiation therapy, or combined surgery and radiation therapy. J Clin Oncol 1999;17:158-67.
2. Enzinger FM, Shiraki M. Musclo-aponeurotic fibromatosis of the shoulder girdle (extra-abdominal desmoid). Cancer 1967;20: 1131-40.
3. Enzinger FM, Weiss SW. Soft tissue tumors. 2nd ed. St. Louis: Mosby; 1988. p. 145-53.
4. Harmon RH. Surgical reconstruction of the paralytic shoulder by multiple muscle transplantations. J Bone Joint Surg Am 1950;32: 583-95.
5. Helfet AJ. Coracoid transplantation for recurring dislocation of the shoulder. J Bone Joint Surg Br 1958;40:198-202.
6. Hunt RTN, Morgan HC, Ackerman LV. Principles in the management of extra-abdominal desmoid. Cancer 1960;13:825-36.
7. McLaughlin HL, Cavallaro WV. Primary anterior dislocation of the shoulder. Am J Surg 1950;80:615-21.
8. Nichols RW. Desmoid tumors; a report of thirty-one cases. Arch Surg 1923;7:227-32.
9. Weiss SW, Goldblum JR. Soft tissue tumors. 4th ed. St. Louis: Mosby; 2001. p. 320-9.

# Snapping scapula caused by abnormal angulation of the superior angle of the scapula

Naomi Oizumi, MD, Naoki Suenaga, MD, and Akio Minami, MD, *Sapporo, Japan*

Snapping scapula (crepitus between the scapula and the chest wall) is not a rare condition; however, it only occasionally becomes painful and disabling. Boinet[1] first described a case of snapping scapula in 1867. The etiology of snapping scapula is classified into two categories: skeletal or soft-tissue abnormalities.[2,5-7] Skeletal abnormalities include varied conditions that lead to scapulothoracic incongruity, such as bone tumors of the scapula or ribs (osteochondromas or exostoses), abnormal anterior angulation of the superior angle of the scapula, Luschka's tubercle, bony prominence of the scapula, omovertebral bone, and malunion after fractures of the scapula or ribs. However, in some cases previously reported,[2,11] it was difficult to find obvious skeletal abnormalities and the clear cause of the symptoms was unknown. There have been many reports that mostly revealed good results of surgical treatment for snapping scapula;[2,3,5-10] however, it is still controversial whether operative treatment is necessary.[11]

We experienced a rare case of snapping scapula caused by an abnormal angulation of the superior angle of the scapula that could be diagnosed with the use of 3-dimensional (3D) computed tomography (CT) and cineradiography. Surgical treatment was performed, and a successful result was achieved.

## CASE REPORT

A 20-year-old woman, a nursing school student, noticed crepitus around the left shoulder during shoulder movement 4 years previously. Motion pain appeared 1 year before admittance. She had been treated conservatively by nonsteroidal anti-inflammatory drugs and physical therapy at another hospital, but the symptoms continued. She had no history of trauma. The initial examination at our hospital revealed obvious snapping of the scapula during active depression of the scapula from the elevated position. She had full range of shoulder motion and no obvious muscle atrophy around the shoulder. The position of the scapula was the same on both sides. Although strength of the serratus anterior muscle was slightly weak because of pain and minor winging of the scapula was shown, no other neurologic abnormalities were found. There were no signs of glenohumeral instability or subacromial impingement. There were also no abnormalities of the cervical spine. Radiographically, no abnormal findings, such as bone tumor or deformity of the scapula or ribs, were found. Magnetic resonance imaging of the shoulder also revealed no abnormal findings of the soft tissues including the rotator cuff. On 3D-CT, the superior angle of the scapula showed an abnormal curvature toward the chest wall on the affected side in contrast with the unaffected side (Figure 1, *A* and *B*). The deformity was more obvious in a sagittal sliced view of the scapula, which was reconstructed from the 3D-CT data (Figure 1, *C* and *D*). Because the exact source of the snapping remained unclear, cineradiography was performed to evaluate the pathomechanism of the snapping. Cineradiography clearly showed that the fourth rib was pushed down by the superior angle of the scapula and then snapped back to the original position during the depression of the scapula from the elevated position. The distance between the fourth and fifth ribs was reduced from 17 to 13 mm when the superior angle of the scapula depressed the fourth rib. The snapping was accompanied by pain at the site of the superior angle (Figure 2, *A* and *B*). From these findings, the patient was diagnosed as having a snapping scapula caused by abnormal anterior angulation of the superior angle of the scapula. Because the pain had become severe despite exercise of the shoulder girdle muscles, partial resection of the scapula was performed 3 months after the first visit. The levator scapulae and rhomboid muscles, which attached to the ridge of the superior angle of the scapula, were detached, and the superior angle was exposed. There were no macroscopic abnormalities of the soft tissues. No bone tumor or tubercle was found at the superior angle of the scapula or the fourth rib. The snapping phenomenon could not be demonstrated by passive motion of the scapula intraoperatively. The angulated part of the superior angle (7.0 × 2.6 cm) was completely removed. The levator scapulae and rhomboid muscles were reattached to the remaining superior angle. No abnormal pathologic findings, such as inflammation, bursa, and tumor, were observed. After the patient used a sling for 2 weeks, active motion of the shoulder was begun. At 2 years 6 months after the operation, snapping and pain were completely gone and the patient was satisfied with the results. Postoperative 3D-CT of the scapula showed a complete resection of the curved area of the superior angle (Figure 3).

From the Department of Orthopaedic Surgery, Hokkaido University School of Medicine.

Reprint requests: Naomi Oizumi, MD, Department of Orthopaedic Surgery, Hokkaido University School of Medicine, Kita-15, Nishi-7, Kita-ku, Sapporo 060-8638, Japan (E-mail: *nao9877@aol.com*).

J Shoulder Elbow Surg 2004;13:115-18



1058-2746/2004/$35.00 + 0

doi:10.1016/S0009-9236(03)00178-2

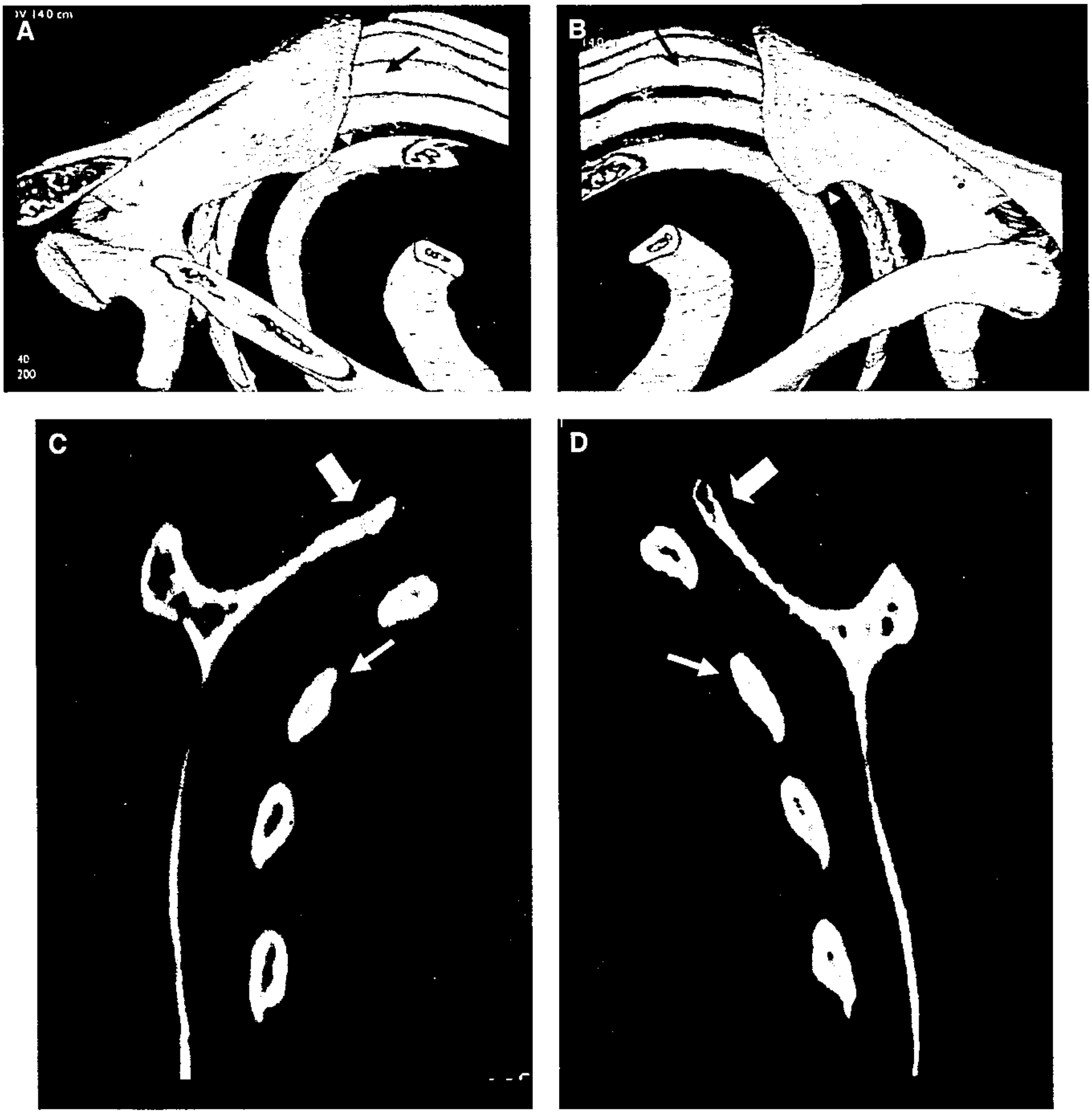


**Figure 1 A** and **B**, Three-dimensional computed tomography (3D-CT) images of the scapula on the right and left sides (superior view), respectively. The *arrowheads* show the superior angle of the scapula, and the *arrow* shows the fourth rib. The superior angle seems to curve toward the chest wall in the left scapula compared with the right side. **C** and **D**, Sagittal view of the scapula reconstructed from 3D-CT data: left (affected) side and right side, respectively. The *wide arrow* shows the superior angle of the scapula, and the *narrow arrow* shows the fourth rib. Clearly, the left superior angle abnormally curves toward the thorax.

## DISCUSSION

In skeletal abnormalities that lead to scapulothoracic incongruity and snapping, osteochondromas or exostoses of the scapula are the most frequent,[2,10] whereas abnormal angulation of the superior angle of the scapula is relatively rare. Milch and Burman[6] first reported 3 cases of snapping scapula with abnormal forward bending of the superior margin of the scapula. Although some authors reported the abnormal angulation of the superior angle of the scapula being diagnosed with plain radiographs,[3,6,7] it is usually

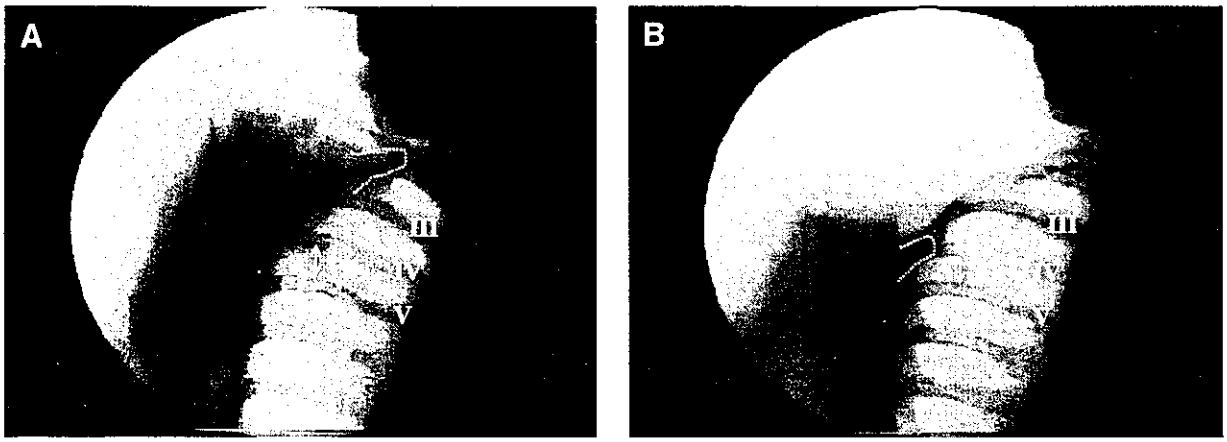


**Figure 2** Cineradiographic image during active elevation and depression of the scapula. The superior angle of the scapula is traced by a *dotted line*. Note that the distance between the fourth and fifth ribs changes because the fourth rib is depressed by the superior angle of the scapula. **A,** The elevated position of the scapula. The distance between the fourth and fifth ribs is 17 mm. **B,** During depression of the scapula, the superior angle of the scapula pushes the fourth rib down, and the distance between the fourth and fifth ribs is reduced to 13 mm.

**Figure 3** Postoperative 3D-CT image of the scapula (sagittal view). The *wide arrow* shows the edge of the removed superior angle of the scapula, and the *narrow arrow* shows the fourth rib. Note that the angulated part of the superior angle is completely resected.

difficult to make a complete evaluation with radiographs only. CT imaging has been used in evaluating some bony abnormalities; however, it was still not sufficient for detecting abnormal angulations of the scapula.[4,9] In the last several years, 3D-CT has been developed to detect more detailed morphologic abnormalities. Mozes et al[9] examined plain radiography, CT, and 3D-CT of 26 patients with snapping scapula and found that only 3D-CT could detect all scapulothoracic incongruities. Harper et al[5] reported 2 cases that showed narrowing between the superomedial border of the scapula and chest wall on 3D-CT. Morse et al[8] reported 1 patient with medial bony prominence of the scapula on 3D-CT. 3D-CT may be able to detect bony abnormalities in some cases of snapping scapula whose causes were unknown in previous studies. In our case, only 3D-CT could detect the abnormal angulation of the superior angle of the scapula. Furthermore, we found the reconstructed sagittal view of the scapula most useful in detecting the deformity, although there are no other reports that have used such a reconstructed sagittal view from 3D-CT.

In most cases the precise site of the scapula at which the snapping occurs is not clear from clinical findings only. Cineradiography has been recommended as a useful method in evaluating the pathomechanism of the snapping scapula; however, to our knowledge, no detailed reports using this method were found. In the present case, cineradiography dynamically visualized the snapping phenomenon accompanied by pain between the superior angle of the scapula and the fourth rib. This finding supported our assumption that the abnormal anterior angulation of the superior angle of the scapula, which was observed on 3D-CT, was the etiology of the patient's symptoms.

Edelson[3] examined 700 dry scapular specimens and reported that the supraspinatus portion of the scapula was bent inward in 8.5% of the samples. This result suggests that it is important to investigate carefully whether the morphologic abnormality is the actual cause of the patient's symptoms before considering treatment. Cineradiography will be helpful to make a definite diagnosis in such cases.

The treatment of the snapping scapula varies according to the etiology. Bone or soft-tissue tumors should be resected; however, it is still controversial whether surgery is necessary in other cases. Most cases with soft-tissue problems have been considered responsive to conservative treatment. Conversely, many authors recommended surgical treatment for patients with obvious bony incongruity between the scapula and the chest wall.[2,3,5-9] There are only a few reports of surgical treatment for abnormal angulation or curvature of the superior angle of the scapula.[3,5,6,9] Partial scapulectomy, which includes resection of the superior angle or medial border of the scapula, has been performed for such patients. Milch and Burman[6] appear to be the first authors to report partial scapulectomy for a patient with abnormal forward bending of the superior margin of the scapula. Edelson[3] reported a case in which he performed removal of the medial suprascapular portion and achieved effective pain relief. Mozes et al[9] reported that conservative treatment failed in 11 of 26 patients and they required partial resection of the scapula. Four patients who underwent resection of the superomedial angle gained complete pain relief and elimination of snapping; however, seven patients who had resection of the whole scapular medial border had persistent pain and snapping after surgery. Harper et al[5] reported 7 patients treated by arthroscopic partial resection of the scapula. In their series, postoperative pain persisted in some patients and a second open procedure was required in one. These reports suggest that inadequate partial resection of the scapula can lead to persistent symptoms. In our case, because we determined the adequate resection area from 3D-CT data preoperatively, sufficient resection of the superior angle of the scapula could be done and an excellent postoperative result was achieved. Furthermore, we consider that the repair of the muscles that attach to the superior angle, such as levator scapulae and rhomboid muscles, is important to achieve a successful result.

## REFERENCES

1. Boinet. (Case presentation) Bulletin de la Societe Imperiale de Chirugie de Paris, 2me Serie 1867;8:458.
2. Carlson HL, Haig AJ, Stewart DC. Snapping scapula syndrome: three case reports and an analysis of the literature. Arch Phys Med Rehabil 1997;78:506-11.
3. Edelson JG. Variations in the anatomy of the scapula with reference to the snapping scapula. Clin Orthop 1996;322:111-5.
4. de Haart M, van der Linden ES, de Vet HC, Arens H, Snoep G. The value of computed tomography in the diagnosis of grating scapula. Skeletal Radiol 1994;23:357-9.
5. Harper GD, McIlroy S, Bayley JI, Calvert PT. Arthroscopic partial resection of the scapula for snapping scapula: a new technique. J Shoulder Elbow Surg 1999;8:53-7.
6. Milch H, Burman MS. Snapping scapula and humerus varus. Arch Surg 1933;26:510-85.
7. Milch H. Partial scapulectomy for snapping of the scapula. J Bone Joint Surg Am 1950;32:561-6.
8. Morse BJ, Ebraheim NA, Jackson WT. Partial scapulectomy for snapping scapula syndrome. Orthop Rev 1993;22:1141-4.
9. Mozes G, Bickels J, Ovadia D, Dekel S. The use of three-dimensional computed tomography in evaluating snapping scapula syndrome. Orthopedics 1999;22:1029-33.
10. Parsons TA. The snapping scapula and subscapular exostosis. J Bone Joint Surg Br 1973;55:345-9.
11. Percy EC, Birbrager D, Pitt MJ. Snapping scapula: a review of the literature and presentation of 14 patients. Can J Surg 1988;31:248-50.

# SURGICAL TREATMENT OF ACUTE ELBOW FLEXION CONTRACTURE IN PATIENTS WITH CONGENITAL PROXIMAL RADIOULNAR SYNOSTOSIS

## A REPORT OF TWO CASES

BY TATSUYA MASUKO, MD, HIROYUKI KATO, MD, AKIO MINAMI, MD,
MASAYUKI INOUE, MD, AND TAKAKAZU HIRAYAMA, MD

*Investigation performed at the Department of Orthopaedic Surgery, Hokkaido University School of Medicine, Sapporo, Japan*

Congenital proximal radioulnar synostosis is a rare congenital upper-extremity disorder in which the proximal aspects of the radius and ulna are fused and the rotational motion of the forearm is restricted. It has been estimated that 26% of all patients who have congenital radioulnar synostosis have a 10° to 30° limitation of elbow extension[1]. The Japanese-language literature includes reports on three patients with congenital proximal radioulnar synostosis who had an acute development of elbow flexion contracture[2-4]. However, to our knowledge, there have been no published reports in the English-language literature regarding patients with this disorder. We describe the cases of two boys with congenital proximal radioulnar synostosis in whom an elbow flexion contracture developed in a relatively acute manner. After removal of a hypoplastic lateral soft-tissue structure analogous to the annular ligament, both patients were able to achieve full extension of the elbow without recurrence of the elbow flexion contracture. Our patients and their families were informed that data from the cases would be submitted for publication.

### Case Reports

CASE 1. A thirteen-year-old boy had a restriction in elbow extension after having slept with the elbow held in a hyperflexed position. Three days after this first episode, which had resolved spontaneously, the same elbow flexion contracture appeared without any inducement and continued for seven days, at which point the patient was seen in our clinic. There was no history of trauma, and physical examination demonstrated neither swelling nor ecchymosis of the elbow. The patient had pain in the elbow and was noted to have some tenderness over the right radial head and the anterior aspect of the elbow joint. The active range of motion was from 75° to 135° (Fig. 1-A). The right forearm was fixed in 10° of prona-

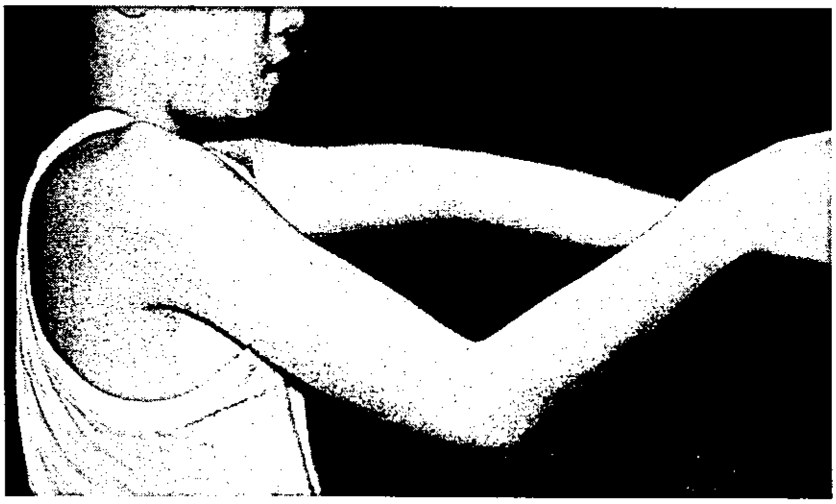

Fig. 1

**Figs. 1-A through 1-H** Case 1. **Fig. 1-A** Preoperative photograph showing that active extension of the right elbow is restricted to –75°.

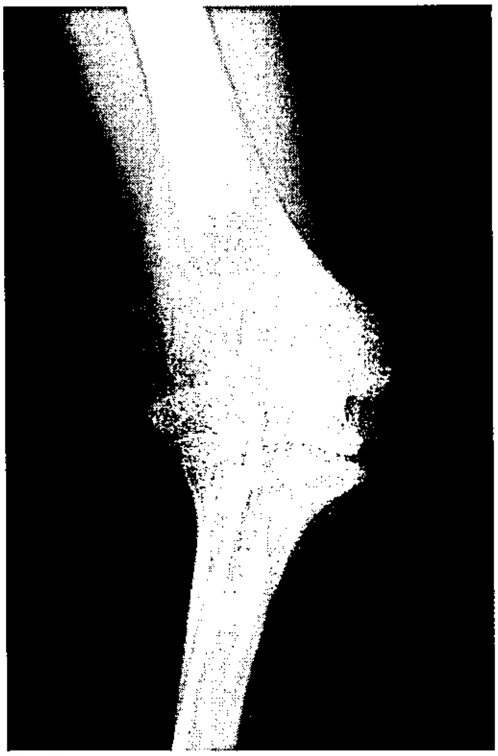

Fig. 1-B

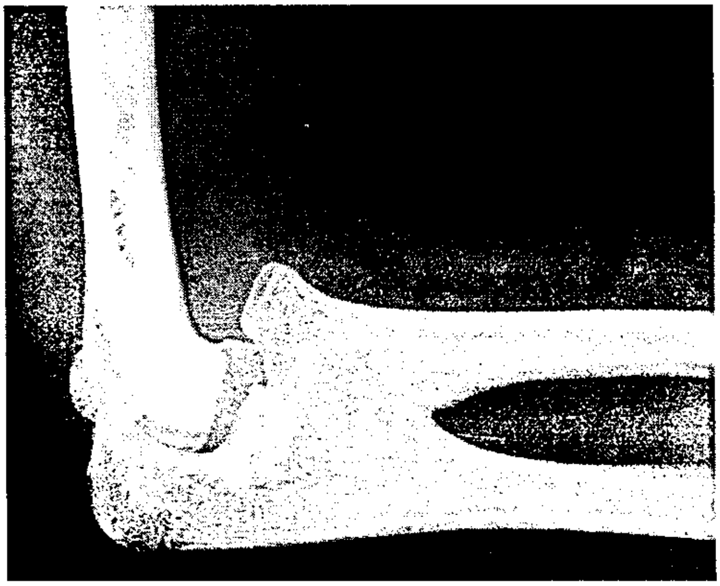

Fig. 1-C

Preoperative anteroposterior (Fig. 1-B) and lateral (Fig. 1-C) radiographs of the right elbow, showing synostosis of the proximal aspects of the radius and ulna. The radial head is displaced anteriorly, consistent with a Type-IV deformity[5].

tion. The patient had been aware of this limitation of forearm rotation since the age of seven years. The active range of motion of the contralateral elbow was from 10° to 150°, with 35° of pronation and 65° of supination. There was no prenatal or family history of any similar disorder. No neurovascular disorder of the upper extremities was detected. The laboratory data were unrevealing. Radiographs revealed bilateral synostosis of the proximal aspects of the radius and ulna (Figs. 1-B and 1-C). A lateral radiograph of the right elbow demonstrated anterior displacement of the radial head, classified as a Type-IV synostosis according to the system of Cleary and Omer[5]. An arthrogram of the right elbow demonstrated that contrast medium did not flow from the humeroradial joint to the space of the sacciform recess beyond the annular ligament (Fig. 1-D). The plain radiographs and the arthrogram did not demonstrate any loose bodies, bone spurs, or incongruity of the joint surface between the humerus and the ulna. Manual mobilization of the elbow following an injection of 5 mL of 1% lidocaine into the joint did not lead to an improved range of motion.

Four weeks after the onset of symptoms, surgery was performed through a lateral approach with the patient under general anesthesia. The extensor carpi radialis longus and the anterior capsule were detached from the anterior aspect of the humerus, and the anterior aspect of the radiohumeral joint was exposed. A structure similar to the annular ligament was noted to overlap the anteriorly dislocated radial head (Figs. 1-E and 1-F). This structure was hypoplastic compared with a normal annular ligament, and it connected to the anterior capsule of the elbow joint. The annular-ligament-like structure was separated from the anterior capsule by incision of the joint capsule, which resulted in a slight improvement of elbow extension to −65°. After the annular-ligament-like structure was excised, it was possible to extend the elbow fully. Histolog-

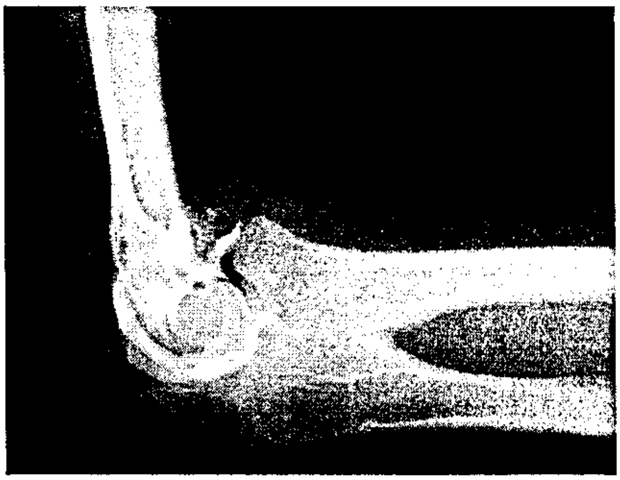

Fig. 1-D

Fig. 1-D Arthrogram of the right elbow, showing that the contrast medium did not flow from the humeroradial joint to the sacciform recess beyond the annular ligament.

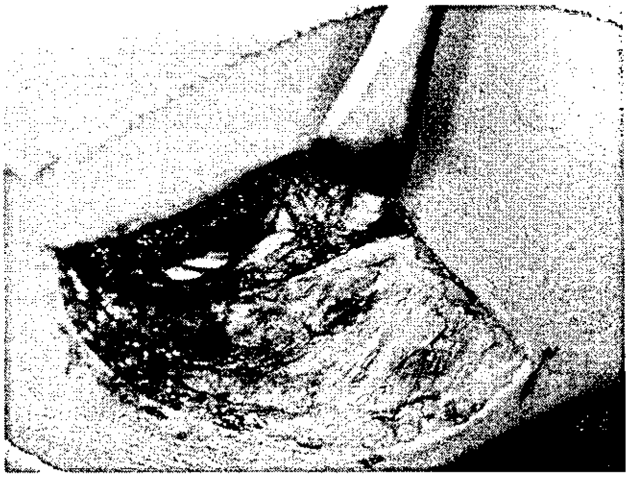

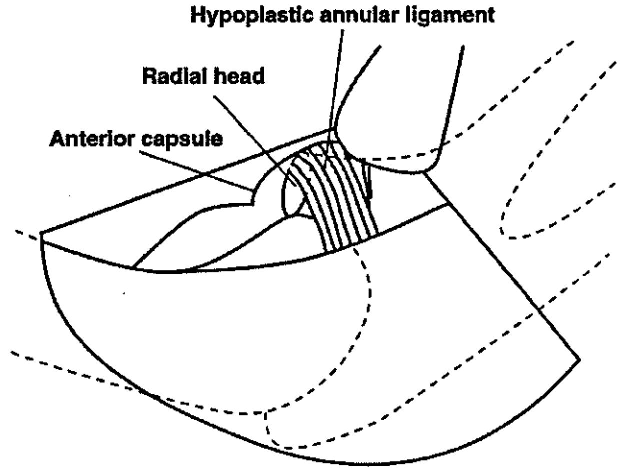


Fig. 1-E

Fig. 1-F

Intraoperative photograph (Fig. 1-E) and line drawing (Fig. 1-F) depicting the annular-ligament-like structure overlapping the radial head, which was dislocated anteriorly. The annular-ligament-like structure was noted to restrict extension of the elbow.

ical examination of the excised specimen revealed collagenous tissue with increased vascularity and no evidence of synovial tissue (Fig. 1-G). Three years after surgery, the active range of motion of the right elbow was from 0° to 150° (Fig. 1-H).

CASE 2. A twelve-year-old boy who had been diagnosed with congenital radioulnar synostosis at the age of nine months presented to our clinic with a flexion contracture of the left elbow. The patient reported that the elbow had been forced into hyperflexion while he had been playing and that he had not been able to extend the elbow fully thereafter. Physical examination revealed that the range of elbow motion was from 50° to 140° (Fig. 2-A). The left forearm was fixed in a neutral position. No neurovascular disorder was noted. Radiographs of the left elbow showed synostosis of the proximal metaphyses of the radius and ulna (Figs. 2-B and 2-C). The left radial head was dislocated anteriorly and was classified as a Type-IV synostosis according to the system of Cleary and Omer[5]. Surgery was performed forty days after the onset of the flexion contracture. The operative procedure was essentially the same as that performed in the first patient (Case 1). The lateral part of the annular-ligament-like structure was connected to the humeral origin of the collateral ligament. When the elbow was ex-

Fig. 1-G
Photomicrograph of the excised specimen, showing collagen fibers (arrow) and increased vascularity throughout the tissue. No synovial tissue is evident (original magnification, ×100).

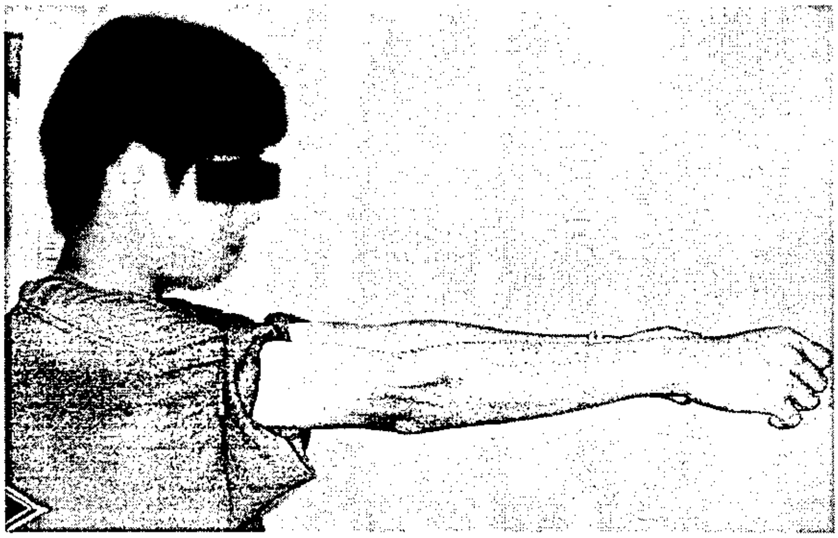

Fig. 1-H
Photograph made three years after surgery, showing full extension of the right elbow.

tended, this structure became caught on the radial head. We excised the anterior portion of the annular-ligament-like structure, preserving the lateral collateral ligament. Subsequently, the limitation of elbow extension resolved completely. At the twelve-year follow-up evaluation, the patient reported that there had been no recurrence of pain, restriction of movement, or flexion contracture of the elbow.

### Discussion

Acute episodes of elbow locking are usually secondary to loose bodies resulting from osteochondritis dissecans[6,7], synovial osteochondromatosis[8], or osteoarthritis[9,10]. A search of the English-language literature revealed no previous reports of acute elbow flexion contracture developing in association with congenital proximal radioulnar synostosis. A search of the Japanese-language literature revealed three cases[2-4].

The three previous Japanese patients and the two patients described in the present report had similar clinical and radiographic characteristics (Table I). All five patients were male, and all but one were twelve to sixteen years old at the time of the acute flexion contracture episode. In all five patients, the episode of contracture was induced by a common trigger, specifically, forced hyperflexion of the elbow. All of the contractures appeared to be caused by an abnormal anatomical relationship among the annular-ligament-like structure, the anterior capsule, and the radial head. All five injuries were

**TABLE I Reported Cases of Elbow Flexion Contracture in Patients with Congenital Proximal Radioulnar Synostosis**

| | Gender, Age (yr) | Classification[5]* | Pathogenesis of Contracture | Operative Procedure | Operative Result | Duration of Follow-up |
|---|---|---|---|---|---|---|
| Kikuchi et al.[2] | M, 16 | Type IV | Hypertrophic anterior capsule | Excision of the anterior capsule, excision of the radial head | No contracture | 2 yr, 2 mo |
| Kurihara et al.[3] | M, 24 | Type IV | Annular-ligament-like structure | Excision of the annular-ligament-like structure, excision of the radial head | No contracture | 1 yr, 4 mo |
| Takamine et al.[4] | M, 12 | Type IV | Annular-ligament-like structure, hypertrophic anterior capsule | Excision of the annular-ligament-like structure, excision of the anterior capsule | No contracture | 4 mo |
| Present report | | | | | | |
| Case 1 | M, 13 | Type IV | Annular-ligament-like structure | Excision of the annular-ligament-like structure | No contracture | 3 yr |
| Case 2 | M, 12 | Type IV | Annular-ligament-like structure | Excision of the annular-ligament-like structure | No contracture | 12 yr |

*Type IV = radial head dislocated anteriorly.

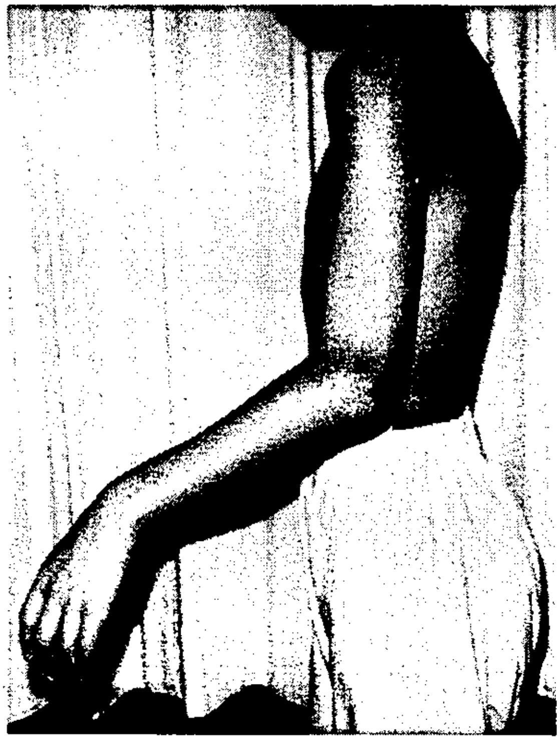

Fig. 2-A

**Figs. 2-A, 2-B, and 2-C** Case 2. **Fig. 2-A** Preoperative photograph showing that active extension of the elbow is restricted to −50°.

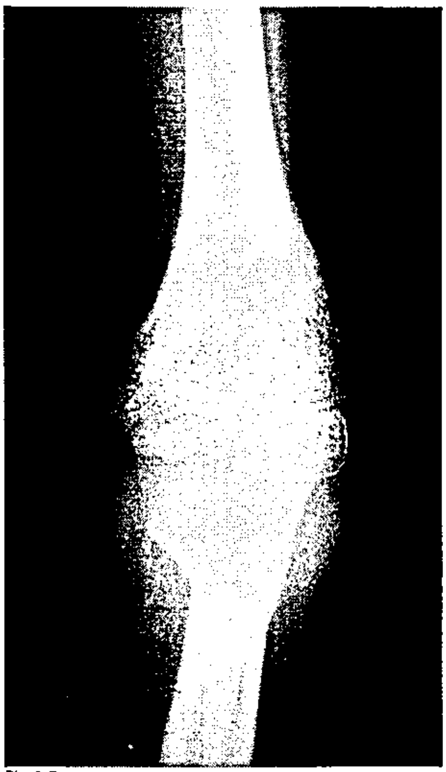

Fig. 2-B

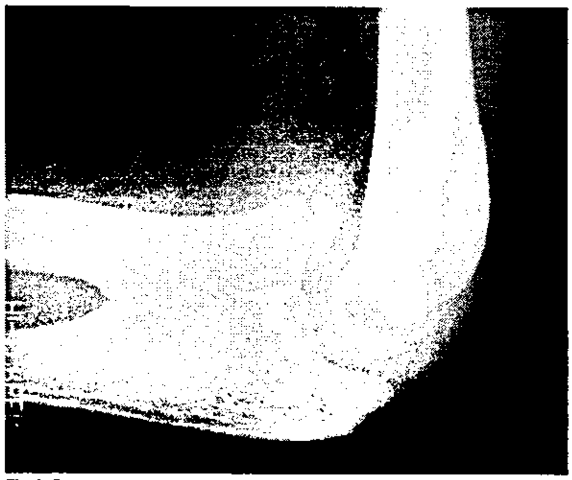

Fig. 2-C

Preoperative anteroposterior (Fig. 2-B) and lateral (Fig. 2-C) radiographs showing a synostosis of the proximal ends of the left radius and ulna. The left radial head is displaced anteriorly, consistent with a Type-IV deformity[5].